

## Direct Abstraction of Surface-Bound Hydrogen on Ni(111) by Free Methyl Radicals

Miguel E. Castro,<sup>†,‡</sup> Richard B. Hall,<sup>\*,§</sup> and Charles A. Mims<sup>\*,†</sup>

Corporate Research Laboratories, Exxon Research and Engineering Company, Clinton Township, Route 22 East, Annandale, New Jersey 08801, and Department of Chemical Engineering and Applied Chemistry, 200 College Street, University of Toronto, Toronto, Ontario, Canada M5S3E5

Received: May 2, 1997; In Final Form: July 2, 1997<sup>®</sup>

Methane (CH<sub>3</sub>D) is formed directly by abstraction by methyl radicals of adsorbed D on a Ni(111) surface. This reaction occurs at a surface temperature of 120 K and in the presence of open metal binding sites. A direct reaction by unaccommodated methyl radicals is involved, since accommodated methyl radicals on Ni(111) react only above 200 K. Modeling efforts show that the cross section for accommodation of methyl radicals to open metal sites is approximately five times larger than that for D abstraction.

The surface reactions of hydrocarbon radicals are important in a large number of catalytic reactions, and extensive investigations have revealed many important details of these reaction steps.<sup>1–3</sup> Because of their role in methane conversion reactions and hydrocarbon synthesis, and because they are the simplest of the alkyl species, methyl radicals have received a large share of this attention. The formation of methane from adsorbed CH<sub>3</sub> and H fragments on nickel surfaces is a significant step in C<sub>1</sub> chemistry on nickel and has been extensively studied both experimentally and theoretically.<sup>1,4–16</sup> Considerable complexity has been revealed in ultrahigh vacuum (UHV) studies of this simple reaction. Coadsorbed CH<sub>3</sub> and D produces methane near 250 K on both the Ni (100) and Ni(111) surfaces. Although CH<sub>3</sub>D is the predominant product on Ni(100), only minor quantities are produced on Ni (111) while larger amounts of CH<sub>4</sub> desorb near 250 K during temperature-programmed desorption (TPD) in a complex series of processes requiring two methyl species.<sup>4</sup>

The reactions of surface-bound species, prepared by various methods, dominate these investigations and undoubtedly make up the majority of reaction steps in the catalytic reactions. However, the surface reactions of free radicals are also significant in several important catalytic processes. The surface reactions of free methyl radicals are significant in methane oxidative coupling<sup>17</sup> and other catalytic systems that involve simultaneous homogeneous and heterogeneous chemistry.<sup>18–21</sup> Surface reactions of activated intermediates are also significant in chemical vapor deposition and plasma etching where energetic species, generated elsewhere, impinge on the surface. The role of methyl radicals in diamond film growth has received substantial attention.<sup>22,23</sup> Free radicals and other surface reactants with excess energy, i.e., those that have not formed stable, thermally equilibrated bonds to available unoccupied binding sites, are capable of participating in reaction channels which are inaccessible once such bonding occurs.<sup>24–33</sup> To be significant in the presence of unoccupied binding sites, such “hot” reaction channels must compete with the very rapid rates of energy transfer on solid surfaces. This Letter provides direct evidence that free methyl radicals can efficiently abstract surface H from Ni(111) at low surface temperatures (120 K), in

competition with the formation of surface Ni–CH<sub>3</sub> bonds on unoccupied nickel metal sites.

The experiments were carried out in an ultrahigh vacuum chamber<sup>4,34</sup> with a base pressure below 10<sup>–10</sup> Torr, which is equipped for TPD and residual gas analysis (RGA) measurements, Auger electron spectroscopy (AES), and low-energy electron diffraction (LEED). The gas-phase methyl free radical source, in which azomethane is pyrolyzed in the dosing gas delivery tube, was made of alumina heated by an external winding of tantalum wire and patterned after the source described in refs 35 and 36. The Ni(111) crystal was spot-welded to tantalum wires for resistive heating to 1200 K and could be cooled to 110 K with liquid nitrogen. A chromel–alumel thermocouple was also welded to the side of the crystal. Repeated cycles of Ne<sup>+</sup> ion bombardment (5 min) and annealing at 1000 K (10 min) were used for initial surface cleaning. Residual surface carbon contamination was removed by sequential 1 L doses of O<sub>2</sub> and H<sub>2</sub>, each followed by heating to 900 K; this cycle was repeated until no impurities were detected by AES. Azomethane was prepared as described in ref 37 and stored in stainless steel bombs. It was purified prior to each use by several freeze–pump–thaw cycles. The source was not differentially pumped, and the dosing gas, consisting of methyl radicals, ethane, nitrogen, hydrogen, and minor amounts of methane and other species, was largely equilibrated to the room-temperature walls of the vacuum chamber. Results obtained with the crystal in front of the doser were similar to those obtained with the crystal withdrawn into the side of the chamber. MS analyses of the dosing gas were based on spinning rotor gauge calibrations of the permanent gases and the measured fragmentation patterns. The remaining (substantial) intensities at *m/e* = 15, 14, 13 were used to calculate the CH<sub>3</sub> mole fraction (15% at our standard 1 × 10<sup>–8</sup> Torr dosing pressure) assuming the same ionization cross section for CH<sub>3</sub> and CH<sub>4</sub>. Calculated Knudsen impingement rates provide an estimate of the methyl radical flux at this dosing pressure to be 1.5 (+0.6, –0.4) × 10<sup>12</sup> cm<sup>–2</sup> s<sup>–1</sup>. The methyl radical mole fraction was substantially lower if the source was operated at higher pressures, due to the increased probability of recombination reactions. Dosing of deuterium was performed with the surface temperature held at 200 K, while CH<sub>3</sub>(g) was dosed with the sample cooled to 120 K. TPD analyses were performed at 3 K/s, and coverages ( $\theta$ ) in this study refer to the surface Ni density ( $\theta$  = 1, 1 monolayer (ML) = 1.9 × 10<sup>15</sup> cm<sup>–2</sup>). The TPD yields were calibrated against reference systems as described in ref 5.

The production of methane at 120 K by direct reaction of

\* To whom correspondence should be addressed.

<sup>†</sup> University of Toronto.

<sup>‡</sup> Permanent address: The University of Puerto Rico, Department of Chemistry, Mayaguez, Puerto Rico.

<sup>§</sup> Exxon Research and Engineering Company.

<sup>®</sup> Abstract published in *Advance ACS Abstracts*, September 15, 1997.

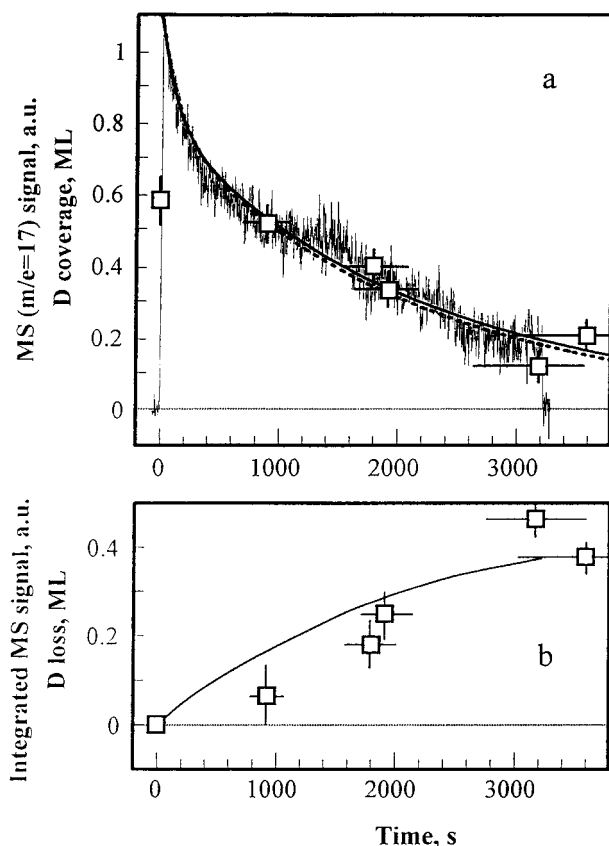


**Figure 1.** Abstraction of adsorbed D from D(0.58)/Ni(111) by gas-phase methyl radicals at a total dosing pressure of  $10^{-8}$  Torr, surface temperature = 120 K. Panel a: trace = MS signal ( $m/e = 17$ ,  $\text{CH}_3\text{D}$ ) during  $\text{CH}_3(\text{g})$  exposure, data points =  $\theta_{\text{D}}(\text{D}/\text{Ni})$  determined by TPD after  $\text{CH}_3$  exposure for the indicated times. Simulation results using parameters in Table 1 are shown as a heavy solid line (model I) and heavy dashed line (model II). Panel b: solid line = integrated MS  $\text{CH}_3\text{D}$  signal,  $\theta_{\text{D}}$  data from (a) expressed as a loss in  $\theta_{\text{D}} = \theta_{\text{D}}(t=0) - \theta_{\text{D}}(t)$ . Indicated uncertainties in dosing time reflect uncertainties in dosing pressure.

methyl radicals with preadsorbed surface deuterium is shown in Figure 1. Figure 1a shows the RGA trace of mass 17 ( $\text{CH}_3\text{D}$ ) during the exposure of the Ni(111) surface, precovered with 0.68 ML ( $1.1 \times 10^{15} \text{ cm}^{-2}$ ) of D to the  $\text{CH}_3$  source. The initial rate of  $\text{CH}_3\text{D}$  formation decreases rapidly for the first few hundred seconds and then continues with slowly decreasing rate. By the end of this experiment, there were approximately 3.0 methyl impingements per surface nickel atom. That the product arises from the Ni(111) crystal is confirmed by the absence of  $\text{CH}_3\text{D}$  in control experiments in which the deuterium adlayer was flashed to 400 K to remove D from the crystal only. Furthermore, the integrated amount of  $\text{CH}_3\text{D}$  is consistent with the amount of D removed from the surface (see below). The high background of ethane from the source precluded our observation of any ethane that might have been formed by methyl radical combination on the surface during this experiment. Similarly, methyl radicals that may have rebounded from the surface were undetectable. Analyses of the surface adlayer by TPD after several various exposure times to the methyl radical source provides an independent measure of the D abstraction rate. The remaining surface deuterium, which evolves in TPD as methane (near 250 K) and in molecular hydrogen (300–450 K), decreases with increasing methyl exposure (data points in panel a). The deuterium loss curve obtained by integrating the  $\text{CH}_3\text{D}$  production rate is shown in Figure 1b. Precise calibration of the rates is difficult because of pumping speed uncertainties during the methyl dose, so the

integral in Figure 1b is simply scaled to agree with the TPD analysis of the overall loss of D(a), also shown in Figure 1b. Nevertheless, attempts at calibration gave  $\text{CH}_3\text{D}$  yields that are within a factor of 2 of the D lost from the surface. A repetition of the experiment with a significantly higher source pressure proved that the observed processes ( $\text{CH}_3\text{D}$  formation, D abstraction) result from methyl radical reactions and not processes such as scrambling and displacement reactions with the permanent gases. In this experiment, the ratio of methyl radicals to the permanent gases was lower by a factor of 5 and the same processes were observed with yields proportional to the methyl radical exposure. The surface inventory of H observed in TPD could be attributed to that from the reactions of  $\text{CH}_3(\text{ads})$  both by stoichiometry and from previous studies.<sup>4</sup> The lack of  $\text{H}_2$  adsorption is consistent with the low sticking probability of  $\text{H}_2$  on Ni(111) at 120 K (particularly with the partial D adlayer in place).<sup>38</sup>

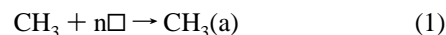
The  $\text{CH}_3\text{D}$  production rate decreases dramatically during the first 500 s, while the surface D coverage decreases little (see Figure 1). The integrated MS signal has a curvature that does not differ significantly from first-order behavior (very little D is lost during the initial high-rate period). This curvature is not resolved in the TPD data, although the agreement is satisfactory. Coverage by surface  $\text{CH}_x$  groups, also obtained in postdose TPD analyses, rises rapidly during the initial period of high rate. The total reaction probability (surface  $\text{CH}_x$  formation plus  $\text{CH}_3\text{D}$  formation) is initially near unity. Subsequently, the  $\text{CH}_x$  uptake increases slowly to backfill the open sites created by  $\text{CH}_3\text{D}$  formation.

The methane production rate is proportional to the surface deuterium during most of the experiment. The deuterium adlayer is distinctly more reactive, however, during the initial phases of the experiment. This could arise from a variety of mechanisms.

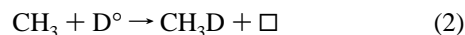
(I) In one interpretation, a small fraction of D is adsorbed on highly reactive (defect, low coordination) sites.

(II) Alternatively, the reactivity of some or all of the deuterium is lower when the surface is filled by the accumulated  $\text{CH}_x$  coadsorbates than when the surface is more open. This could arise through kinematic effects such as shadowing/blocking of D by  $\text{CH}_x$  neighbors, through electronic effects of the adlayer, or from better access to the transition state near an empty site.

Both models can easily fit the data, and the curves in Figure 1a are the results of simple simulations based on the two explanations above. Discrimination among the possibilities require a full investigation outside the scope of this paper. The model here is used to put the competition between D abstraction and methyl accommodation on a semiquantitative basis. Both scenarios can be modeled with three elementary reactions involving the impinging methyl radicals: (1) the formation of a surface bound methyl



where  $\square$  represents an open metal site; (2) reaction with  $\text{D}^\circ$ , surface deuterium characteristic of the reactivity during most of the experiment



and (3) the reaction of  $\text{CH}_3$  with  $\text{D}^*$  (a more reactive type of surface deuterium).

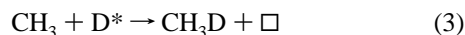


TABLE 1: Parameters Used in Simulations. See Text for Explanation

	Figure 1. D(0.58 ML)/Ni(111)		Figure 2. D(0.58 ML)/C(0.07 ML)/Ni(111) <sup>a</sup>					
			model I <sup>c</sup>			model II		
	model I	model II	+	−	0	+	−	
<i>n</i>	3.3	3.3	3.3	3.3		3.3	3.3	
<i>m</i>						1	3	
$\sigma_1$	2.7	2.7	2.7	2.7		2.7		
$\sigma_2$	0.65	0.60	0.65	0.65	0.7	0.6	0.6	
$\sigma_3$	8	1.3	8	8		1.3		
initial $\theta_{D^*}$ , ML	0.02	0.24 <sup>b</sup>	0.015	0.007	0	0.20 <sup>b</sup>	0.09 <sup>b</sup>	

<sup>a</sup> The fits + represent the maximum contribution of D\* consistent with the data, − represent the minimum, and 0 is the best first-order fit (no D\*). These symbols are consistent with the notation in Figure 2. <sup>b</sup> Calculated from 0.58 (1 −  $\theta_D$  −  $m\theta_C$ ).

Each of these steps is assumed to be a simple first-order process: e.g. for reaction 1

$$r_1 = I_{CH_3} \cdot \theta_{\square} \cdot \sigma_1, \text{ etc.}^4 \quad (4)$$

where  $r$ , the rate, and  $I_{CH_3}$ , the methyl radical impingement rate, are expressed per nickel surface atom. The  $\sigma_i$  are the reaction probabilities upon collision with the appropriate type of site. In the first scenario above (I), D\* and D° represent separate species that react independently with the impinging methyl radicals, and in the second scenario (II), D\* is assumed to be a fraction of the total D adlayer, which is assumed to be determined by the instantaneous number of open sites. In the simulation used in Figure 1,  $\theta_{D^*} = (\theta_{D, \text{total}})\theta_{\square}$  while  $\theta_{D^{\circ}}$  is the remainder. The parameters for the two fits are given in Table 1. The value of  $n$  is obtained from the maximum uptake (0.30 ML) of methyl on the clean surface.<sup>4</sup> The absolute values of the reaction probabilities are uncertain by a factor of 2 or more owing to uncertainty in the CH<sub>3</sub> flux, but the relative values are instructive. Thus, in scenario I, 4% of the initial D has roughly 10 times the reactivity of the rest of the adlayer. In the second scenario, the presence of empty sites makes a portion of the adsorbed D approximately twice as reactive as it is with a crowded surface. In any case, comparison of the CH<sub>3</sub>D yield and the number of adsorbed methyls at the end of the initial period gives an average branching ratio (accommodation/D abstraction) of 1.5 to 2. The average ratio of open sites to D(ads) during this period is  $0.4 \pm 0.05$ ; therefore, the cross section for full accommodation to open sites is 3–6 times larger than abstraction of D. This calculation is consistent with the cross section ratios in Table 1.

The results of an experiment wherein 0.07 ML of carbon was adsorbed prior to 0.55 ML D are shown in Figure 2. The carbon was administered by annealing an ethylene adlayer on the clean surface to 550 K<sup>39</sup> and was analyzed by AES. The figure shows that the high initial rate of CH<sub>3</sub>D production from methyl radicals is attenuated by the carbon coadsorbate but is still apparent in the data. Both models can again provide virtually identical fits to this experiment. These are shown in the figure and the parameters listed in Table 1. The noise in the data precludes a precise analysis of the effect; therefore, two sets of simulations were used to span the range consistent with the data; one (denoted + in the figure and Table 1) contains the maximum contribution of D\* and the other (denoted −) the minimum. Only one fit from each set is shown on the figure since the two models produce indistinguishable results. Also shown in the figure is the best fit first-order decay, i.e., no contribution by D\*. Examination of the parameters in Table 1 shows that, with the same cross sections as before, the effect of the carbon precoverage can be explained by a reduction of the initial D\* coverage (model I) or by accounting for the open sites blocked by carbon (model II). The additional parameter,  $m$ , represents

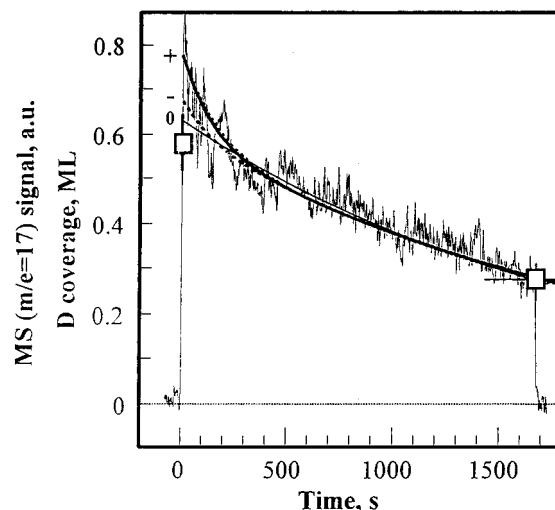


**Figure 2.** Abstraction of adsorbed D from D(0.58 ML)/C(0.07 ML)/Ni(111) by gas-phase methyl radicals at a nominal total dosing pressure of  $10^{-8}$  Torr. Trace = MS signal ( $m/e = 17$ , CH<sub>3</sub>D) during CH<sub>3</sub>(g) exposure, data points =  $\theta_D(D/Ni)$  determined by TPD after CH<sub>3</sub> exposure for the indicated times. The labels to the left of the simulation traces refer to fits consistent with the maximum (+, heavy solid line), minimum (−, heavy dashed line), and zero (0, light solid line) contribution from D\* (see text and Table 1 for parameters). Both models give indistinguishable results for each set.

the number of nickel sites blocked by each preadsorbed carbon atom. Since attenuation of the rapid reaction by coadsorbates is consistent with both interpretations, we cannot discriminate between these explanations. The second explanation inherently links the time scale of the rapid reaction to the disappearance of open sites, which might be supported by further experimentation with a variety of site-blocking adsorbates. In any case, the preadsorbed carbon does not selectively poison any special D adsorption sites.

These results show that CH<sub>3</sub>(g) can abstract hydrogen from a cold Ni(111) surface in direct competition with binding to metal sites. This reaction must, therefore, be a direct and efficient abstraction process. The reaction is substantially exoergic: ( $D_0(Ni(111)-H)$ , 265 kJ/mol<sup>40</sup> −  $D_0(CH_3-H)$ , 435 kJ/mol<sup>41</sup> = −170 kJ/mol). Gas-phase thermoneutral H-abstraction reactions by methyl radicals proceed with energy barriers in the range of 40–50 kJ/mol, and correlations between exoergicities and activation energies<sup>42,43</sup> predict little or no energy barrier for similar reactions with exoergicities greater than approximately 100 kJ/mol.<sup>44</sup> Once complete bonding of the methyl group to the nickel surface ( $D_0(H_3C-Ni) = 160^{12} - 205^{14}$  kJ/mol) occurs, methane formation is approximately thermoneutral and the inherent energy barrier for this process requires higher surface temperatures in order to proceed. An inherent barrier of 40–50 kJ/mol is consistent with the 250 K reaction temperature for methane formation from accommodated

H and CH<sub>3</sub>. In experiments similar to those above, we examined the reactions of methyl radicals with several other preadsorbed species, including C<sub>2</sub>D<sub>6</sub>, D<sub>2</sub>O, and CD<sub>3</sub> groups formed by CD<sub>3</sub>I dissociation. Abstraction of D was not observed from any of these adsorbates, a reflection of the less favorable energetics in these reactions. Furthermore, no detectable ethane (CH<sub>3</sub>CD<sub>3</sub>) was formed from reaction with CD<sub>3</sub>. The lack of detectable products in these experiments implies reaction probabilities smaller than 0.01.

In addition to being supplied from the gas phase, energetic radicals on the surface can also result from prior reaction steps in which substantial amounts of energy are released. For example, energetic surface alkyl radicals prepared by reaction of gas-phase H radicals and adsorbed alkenes<sup>25</sup> show unusual reactivity. Free methyl radicals have been observed during the dissociation of methyl halides on copper<sup>45</sup> and silver single-crystal surfaces.<sup>46</sup> Other cases of methyl radical liberation have been reported from the dissociation of other precursors.<sup>47</sup> On Ni(111)<sup>5,8,10</sup> methane (CH<sub>3</sub>D) forms from coadsorbed CH<sub>3</sub>I and D at much lower temperatures (150 K) than the 250 K required for coadsorbed CH<sub>3</sub> and D. This methane forms coincidentally with C–I bond scission, and although free methyl radicals are not detected in this process, we have argued that the methane arises from the reaction of energetic, unaccommodated methyl radicals.<sup>5</sup> Simulations of this process required the cross section for accommodation to be five times the cross section for methane formation—a value in good agreement with the current results (see Table 1).

Direct surface reaction steps that do not require preadsorption as a surface precursor (known in catalysis as Eley–Rideal mechanisms) have been observed in surface-molecular beam experiments involving hydrogen atoms.<sup>29–31</sup> The reaction of D(g) with adsorbed methyl on Cu(111) shows direct repulsive release of methane,<sup>31</sup> and it is possible that such behavior occurs here. Nevertheless, adsorption in precursor states (not fully accommodated) is likely. Such behavior has been well documented in other systems.<sup>48</sup> The CH<sub>3</sub> uptake curve on the clean surface shows some evidence of precursor kinetics (unit sticking probability to high coverage),<sup>4</sup> and trapping the methyl radical in a precursor state requires very little energy loss. The overall energetics are favorable enough to ensure that methyl radicals that are partially accommodated to the surface have the high reaction probabilities implicated here and during methyl iodide dissociation.<sup>5</sup>

**Acknowledgment.** C.A.M. acknowledges support from the Natural Sciences and Engineering Research Council (Canada) and Exxon Research and Engineering Company.

## References and Notes

- (1) For an excellent and exhaustive recent review, see: Bent, B. E. *Chem. Rev.* **1996**, 96, 1361 and other articles in this volume.
- (2) White, J. M. *Langmuir* **1994**, 10, 3946.
- (3) Zaera, F. *Acc. Chem. Res.* **1992**, 25, 260.
- (4) Hall, R. B.; Castro, M. E.; Kim, C.; Mims, C. A. *Proceedings of the 11th International Congress on Catalysis*, Baltimore, MD; Studies in Surface Science and Catalysis 101; Elsevier Science: Amsterdam 1996; p 327.
- (5) Castro, M. E.; Chen, J. G.; Hall, R. B.; Mims, C. A. *J. Phys. Chem.*, in press.
- (6) Yang, Q. Y.; Maynard, K. J.; Johnson, A. D.; Ceyer, S. T. *J. Chem. Phys.* **1995**, 102, 7734.
- (7) Johnson, A. D.; Daley, S. P.; Utz, A. L.; Ceyer, S. T. *Science* **1992**, 257, 223.
- (8) Tjandra, S.; Zaera, F. *J. Am. Chem. Soc.* **1992**, 114, 10645.
- (9) Tjandra, S.; Zaera, F. *Langmuir* **1992**, 8, 2090.
- (10) Tjandra, S.; Zaera, F. *J. Catal.* **1994**, 147, 598.
- (11) Zhou, X. L.; White, J. M. *Surf. Sci.* **1988**, 194, 438.
- (12) Yang, H.; Whitten, J. W.; Thomas, R. E.; Rudder, R. A.; Markunas, R. J. *Surf. Sci.* **1992**, 277, L95.
- (13) Yang, H.; Whitten, Y. L. *Surf. Sci.* **1991**, 255, 193.
- (14) Burghgraef, H.; Jansen, A. P. J.; van Santen, R. A. *Surf. Sci.* **1995**, 324, 345.
- (15) Siegbahn, P. E. M.; Panas, I. *Surf. Sci.* **1990**, 240, 37.
- (16) Sheng, C.; Apeloig, Y.; Hoffmann, R. *J. Am. Chem. Soc.* **1988**, 110, 749.
- (17) Amenomiya, Y.; Birss, V. I.; Galuszka, T.; Sanger, A. R. *Catal. Rev.—Sci. Eng.* **1990**, 32, 163.
- (18) Baldwin, T. R.; Burch, R.; Squire, G. D.; Tsang, S. C. *Appl. Catal.* **1991**, 74, 137.
- (19) Pak, S.; Smith, C. E.; Rosynek, M. P.; Lunsford, J. H. *J. Catal.* **1997**, 165, 73.
- (20) Xie, S.; Ballinger, T. H.; Rosynek, M. P.; Lunsford, J. H. *Stud. Surf. Sci. Catal.* **1996**, 101A, 711.
- (21) Burwell, R. L., Jr. *Chemtracts: Anal., Phys., Inorg. Chem.* **1990**, 2, 58.
- (22) Clark, M. M.; Raff, L. M.; Scott, H. L. *Phys. Rev. B* **1996**, 54, 5914.
- (23) Lee, S.S.; Minsek, D. W.; Vestyck, D. J.; Chen, P. *Science* **1994**, 263, 1596.
- (24) Harris, J.; Kasemo, B. *Surf. Sci. Lett.* **1981**, 105, L281.
- (25) Teplyakov, A. V.; Bent, B. E. *J. Chem. Soc., Faraday Trans.* **1995**, 91, 3645. Contains a mini-review of relevant UHV work through mid-1995.
- (26) Xi, M.; Bent, B. E. *J. Vac. Sci. Technol.* **1992**, B10, 2440.
- (27) Xi, M.; Bent, B. E. *J. Phys. Chem.* **1993**, 97, 4168.
- (28) Yang, M.-X.; Bent, B. E. *J. Phys. Chem.* **1996**, 100, 822.
- (29) Rettner, C. T.; Auerbach, D. J. *Science* **1994**, 263, 365.
- (30) Rettner, C. T.; Auerbach, D. J.; Lee, J. J. *Chem. Phys.* **1996**, 105, 10115.
- (31) Rettner, C. T.; Auerbach, D. J. *J. Chem. Phys.* **1996**, 104, 2732.
- (32) Jachimowski, T. A.; Weinberg, W. H. *J. Chem. Phys.* **1994**, 101, 10997.
- (33) Cheng, C. C.; Lucas, S. R.; Gutleben, H.; Choyke, W. J.; Yates, J. T., Jr. *J. Am. Chem. Soc.* **1992**, 114, 1249.
- (34) Hall, R. B.; Mims, C. A.; Hardenbergh, J. H.; Chen, J. G. *Surface Science of Catalysis*; Dwyer, D.; Hoffmann, F., Eds.; American Chemical Society: Washington, DC, 1991.
- (35) Peng, X.-D.; Viswanathan, R.; Smudde, G. H. J.; Stair, P. C. *Rev. Sci. Instrum.* **1992**, 63, 3930.
- (36) Smudde, G. H. J.; Peng, X.-D.; Viswanathan, R.; Stair, P. C. *J. Vac. Sci. Technol.* **1991**, A9, 1885.
- (37) Renaud, R.; Leitch, L. C. *Can. J. Chem.* **1954**, 32, 545.
- (38) Rendulic, K. D.; Winkler, A. *J. Chem. Phys.* **1983**, 79, 5151.
- (39) Koel, B. E.; White, J. M.; Goodman, D. W. *Chem. Phys. Lett.* **1982**, 88, 236.
- (40) Christmann, K.; Schober, O.; Ertl, G.; Neumann, M. *J. Chem. Phys.* **1974**, 60, 4528.
- (41) *Handbook of Chemistry and Physics*, 76th ed.; CRC Press: Boca Raton, FL, 1995.
- (42) Evans, M. G.; Polanyi, M. *Faraday Soc. Trans.* **1938**, 34, 11.
- (43) Johnston, H. S.; Parr, C. J. *J. Am. Chem. Soc.* **1963**, 85, 2544.
- (44) Dean, A. M.; Bozzelli, J. W., to appear in *Combustion Chemistry II*; Gardiner, W. C., Ed.; Springer-Verlag. Contains a recent treatment of gas-phase abstraction reactions.
- (45) Lin J.-L.; Bent, B. E. *J. Phys. Chem.* **1993**, 97, 9713.
- (46) Zhou, X.-L.; Coon, S. R.; White, J. M. *J. Chem. Phys.* **1991**, 94, 1613.
- (47) Zhu, X.-Y.; White, J. M.; Creighton, J. R. *J. Vac. Sci. Technol.* **1992**, A10, 316.
- (48) For an early example (H<sub>2</sub> on W(100)), see: Yates, J. T.; Madey, T. E. *Surf. Sci.* **1971**, 28, 437. For an elegant recent study of O<sub>2</sub> on Al(111), see: Brune, H.; Wintterlin, J.; Trost, J.; Ertl, G. *J. Chem. Phys.* **1993**, 99, 2128. For surface diffusion of methyl in diamond film growth, see ref 22.